ARTICLE

Monitoring the Oxidation of Edible Oils by Fourier Transform Infrared Spectroscopy

F.R. van de Voort*, A.A. Ismail, J. Sedman and **G. Emo**
Department of Food Science and Agricultural Chemistry, Macdonald Campus of McGill University, Ste. Anne de Bellevue, Quebec, H9X 3V9 Canada

Edible fats and oils in their neat form are ideal candidates for Fourier transform infrared (FTIR) analysis, in either the attenuated total reflectance or the transmission mode. FTIR spectroscopy provides a simple and rapid means of following complex changes that take place as lipids oxidize. Safflower and cottonseed oils were oxidized under various conditions, and their spectral changes were recorded and interpreted. The critical absorption bands associated with common oxidation end products were identified by relating them to those of spectroscopically representative reference compounds. The power and utilty of FTIR spectroscopy to follow oxidative changes was demonstrated through the use of "real-time oxidation plots." A quantitative approach is proposed in which standards are used that are spectroscopically representative of oxidative end products and by which the oxidative state of an oil can be defined in terms of percent hydroperoxides, percent alcohols and total carbonyl content. By using either relative absorption as a basis or calibrating on representative standards, FTIR analysis provides a rapid means of evaluating the oxidative state of an oil or of monitoring changes in oils undergoing thermal stress.

KEY WORDS: Alcohols, aldehydes, *cis/trans* double bonds, fats and oils, Fourier transform infrared spectroscopy, free fatty acids, hydroperoxides, oxidation, quality control.

Autoxidation is a major deteriorative reaction affecting edible fats and oils and is a primary concern to processors and consumers from a quality standpoint because the oxidative breakdown products cause marked off-flavors in an oil. Although relatively well understood in general terms, autoxidation is quite complex and variable, depending on oil type and conditions of oxidation (1). A wide range of end products are associated with the autoxidative deterioration of oils at ambient temperatures (2–5), the most important being hydroperoxides, alcohols and aldehydes. Moisture, hydrocarbons, free fatty acids (FFAs) and esters, ketones, lactones, furans and other minor products may also be produced, with the FFAs becoming more important in thermally stressed oil. In addition, there is significant *cis* to *trans* isomerization and conjugation of double bonds in the hydroperoxides formed as an oil oxidizes. The rate of oxidation and the distribution of accumulated products depend strongly on the oil source, fatty acid composition, degree of unsaturation, presence of metal ions and antioxidants, time and thermal stress, making it essential to have reliable means of assessing the oxidative status and of forecasting the oxidative stability of an oil. The American Oil Chemists' Society (AOCS) has a number of official methods to provide an indication of the oxidative status of an oil (6), the most common being the peroxide value (PV), the anisidine value (AV) and the thiobarbituric acid value. These chemical methods, which are largely empirical in nature, measure either the primary or secondary products of oxidation, i.e., hydroperoxides or carbonyl-type compounds.

Our research seeks to develop rapid, general-purpose Fourier transform infrared (FTIR)-based quality control methods for the food industry (7–11). Recently, we have focused on developing simple, rapid methods for oil analysis, as oils in their neat form are ideal candidates for FTIR applications. Methods for the determination of iodine value (12), saponification number (12) and FFA (13) have been developed, and a number of other methods are in the development stage (PV and AV). The rationale for turning to a new version of an old technology, IR, is that FTIR spectrometers have many advantages over conventional dispersive instruments, with more energy throughput, excellent wavenumber reproducibility and accuracy, extensive and precise spectral manipulation capabilities (ratioing, subtraction, derivative spectra and deconvolution) and advanced chemometric software to handle calibration development (7). Because of these advantages, FTIR spectroscopy can provide much more information on the characteristics, composition and/or chemical changes taking place in fats and oils than can be obtained from conventional dispersive IR instruments. Furthermore, from a practical viewpoint, FTIR quantitative analysis methods are generally rapid (1–2 min), can be automated and reduce the need for solvents and toxic reagents associated with wet chemical methods for fats and oils analyses, making the development of FTIR methods timely in view of present efforts to eliminate toxic solvents (14).

Neat oils applied directly onto a multiple-pass attenuated total reflectance (ATR) crystal or pumped through a transmission flow cell provide high-quality spectra. Solid fats can be handled analogously with an accurately thermostated ($\approx\pm0.2$°C) ATR crystal or flow cell heated to a temperature above the melting point of the fat. Fats and oils, being relatively simple molecular systems composed primarily of triglycerides, exhibit fairly uncomplicated spectra. Most of the important absorption bands lie in the range of ≈3500 to 800 cm^{-1}, a region where most of the more rugged transmission window/ATR materials transmit.

The overall objective of the present work is to lay the foundation for the development of FTIR methods for assessing oil quality in relation to lipid oxidation and thermal stress (e.g., frying oils). A prerequisite to using FTIR spectroscopy to assess the various end products of lipid oxidation is a basic understanding of the spectral changes taking place as an oil oxidizes. Fundamental IR characterization and identification of specific products formed from the oxidation of individual fatty acids and the decomposition of fatty acid hydroperoxides has been done (15,16), but there have been no comprehensive FTIR spectroscopic investigations of edible oils undergoing oxidation. Thus, there is a need to characterize the spectral changes occurring as oil

*To whom correspondence should be addressed at Department of Food Science and Agricultural Chemistry, Macdonald Campus of McGill University, Box 187, Ste. Anne de Bellevue, Quebec, H9X 3V9 Canada.

oxidation proceeds, assign wavelengths to the more common molecular species produced and assess potential spectral cross interferences so that a generalized approach to monitoring and quantitating key products associated with oxidation can be developed. This paper describes the FTIR spectral techniques used to follow the main chemical events occurring as oils oxidize, develops a means by which such events can be tracked on a relative basis and lays the foundation for a quantitative approach to measuring lipid oxidation.

EXPERIMENTAL PROCEDURES

Instrumentation. The instrument used for this work was a Nicolet 8210 FTIR spectrometer (Nicolet Instrument Inc., Madison, WI), run under a DX operating system (17). To minimize water vapor and CO_2 interferences, the instrument was purged with air from a Balston dryer (Balston, Lexington, MA). A heated horizontal ATR sampling accessory, equipped with 40 and 45° ZnSe crystals, and a 90 μ CaF_2 flow cell were used in this study. All spectra were collected from 512 scans at a resolution of 4 cm^{-1} and a gain of 2.0. For oil oxidation monitoring experiments, the Nicolet spectrometer was programmed with macro-command language (12) to automatically record spectra at specified time intervals, to abstract absorbance values (peak height) at pre-selected frequencies and to print the results for each spectrum taken. The time/absorbance data matrix was then entered into a standard graphics program to produce "real-time oxidation plots."

Samples/oxidation. Commercial safflower and cottonseed oil, obtained from a local retail outlet, were used as the base materials for the oxidation studies. Fifty grams of each oil was poured into a 500-mL fritted funnel, packed with activated silica gel (60–200 mesh; Aldrich, Milwaukee, WI), and eluted with 200 mL hexane to remove any oxygenated compounds from the oil, and the solvent was removed from the eluent on a rotary evaporator under reduced pressure. The oil purified by this procedure was used as a reference oil. The efficiency of this procedure in removing hydroperoxides and carbonyl compounds was assessed by carrying out the PV and AV tests (6) on the unpurified and purified oils; PV was reduced from 2–6 to <1.0, and AV from 2–3 to <1.0, by the purification step. An FTIR procedure was devised as a convenient test for the presence of residual alcohols. For this test, 100 μL of deuterium oxide (D_2O) was added to a 2-mL aliquot of the purified sample to exchange any OH groups, thereby shifting their absorptions to lower frequency; ratioing the spectrum of the untreated portion of the oil against that of the D_2O-treated portion then allows the hydroxyl absorptions in the spectrum of the untreated oil to be clearly observed, without spectral interference from the absorptions of the base oil.

Two sets of oxidation experiments were carried out, one at lower temperatures (70–75°C) with a heated ATR crystal and another at higher temperatures (100, 130 and 230°C) with a CaF_2 flow cell. For the ATR work, 1 mL of a fresh oil sample was pipetted onto the crystal (surface area ≈8 cm^2), and its single-beam spectrum was recorded and ratioed against a single-beam spectrum of air (clean crystal surface). Single-beam spectra were subsequently recorded at 0.5-h intervals from this sample as it oxidized on the ATR crystal and were automatically ratioed against the single-beam spectrum of the fresh oil recorded at t = 0. For the higher-temperature oxidation, a reservoir of oil (≈100 mL) was placed in a heating mantle, with the oil temperature adjusted with a rheostat. A positive-displacement piston pump (FMI Lab Pump Model QG50, Oyster Bay, NY) was used to circulate the oil (≈3 mL/min) from the reservoir through the CaF_2 flow cell. A single-beam spectrum of the oil was collected as soon as the temperature of the reservoir equilibrated to operating temperature (defined as t = 0). Subsequently, dry air was bubbled continuously through the oil @ ≈3 mL/min, and single-beam spectra were recorded every 0.5 h and ratioed against the spectrum recorded at t = 0.

Oxidation reference spectra. Commercially available olive oil was spiked with compounds selected as spectroscopically representative of primary and secondary products of oxidation, including (i) oleic acid, (ii) *t*-butyl hydroperoxide, (iii) hexanal, (iv) *trans*-2-hexenal, (v) *trans, trans*-2,4-decadienal, (vi) hexanol and (vii) *trans*-4-hexen-3-one (Aldrich Chemicals), all added at a level of 2% (w/w). A water-saturated sample (≈0.02%) was prepared by adding 1% water to olive oil, shaking and centrifuging (≈10,000 × *g*) to remove residual free water. Spectra of these spiked samples were recorded on a 40° ATR crystal at room temperature and ratioed against the spectrum of the unspiked olive oil to develop a spectral library. This library was used to assign the characteristic absorption bands of key functional groups of compounds that may accumulate in oils undergoing oxidation.

RESULTS AND DISCUSSION

The concept of spectral ratioing. One of the fundamental strengths of FTIR spectroscopy lies in its ability to accurately ratio spectra, allowing one to see small differences that normally might not be apparent in the raw spectrum. The concept of spectral ratioing arises in FTIR spectroscopy because most FTIR spectrometers are single-beam instruments. Thus, the single-beam spectrum recorded for a sample (I_S) consists of the emittance spectrum of the source on which are superimposed the absorptions of the sample as well as of air in the optical path. To eliminate the contributions of the source and the air background, the single-beam spectrum of the sample is digitally ratioed against a single-beam spectrum recorded with no sample in the beam (I_0), yielding the absorbance spectrum of the sample [$A_S = -\log(I_S/I_0)$]. Alternatively, the single-beam spectrum of the sample may be ratioed against the single-beam spectrum of a reference (I_R), thereby eliminating the spectral features common to the sample and the reference in addition to the contributions from the source and air background. This operation [$A_S^r = -\log(I_S/I_R)$] is equivalent to a 1:1 subtraction of the reference spectrum ratioed against an air background from the sample spectrum ratioed against the same background ($A_S - A_R$), but requires only a single mathematical manipulation, i.e.,

$$A_S - A_R = -\log(I_S/I_0) - [-\log(I_R/I_0)] = -\log(I_S/I_R) = A_S^r \quad [1]$$

Figure 1a illustrates the absorbance spectrum of olive oil in its neat form on an ATR crystal, obtained by

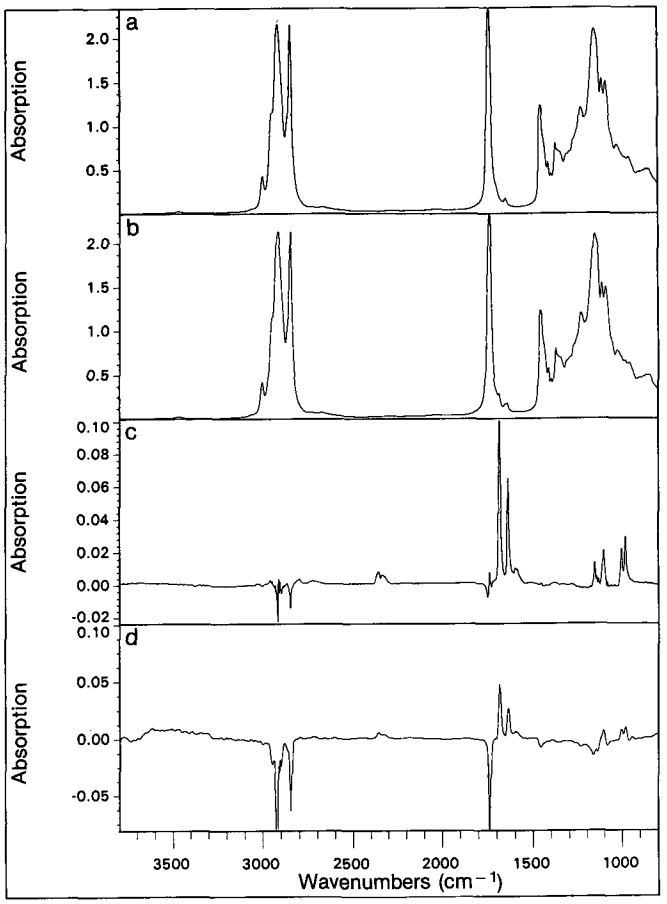

FIG. 1. Attenuated total reflectance/Fourier transform infrared spectra of olive oil (a) and olive oil spiked with 0.5% *trans,trans*-2,4-decadienal (b) on a 40° ZnSe crystal, the difference spectrum obtained by ratioing the single-beam spectrum of the spiked sample against that of the pure olive oil (c) and the corresponding difference spectrum for a 45° ZnSe crystal (d).

ratioing the single-beam spectrum of the oil against the single-beam spectrum of air (bare crystal surface). This spectrum illustrates the dominant spectral features associated with edible oils: the CH stretching absorptions in the region from 3050 to 2800 cm^{-1} (*cis*-C=CH, CH_2, CH_3 and CH_2/CH_3 stretching bands), the carbonyl absorption of the triglyceride ester linkage at 1744 cm^{-1}, and the bands associated with the fingerprint region (1500–1000 cm^{-1}). In a hydrogenated oil, an additional strong band is observed in the 975–965 cm^{-1} region due to the C=C-H bending vibration of *trans* double bonds; measurement of this absorption band in the IR spectrum is the basis for the AOCS official method for the determination of isolated *trans* groups (6). Figure 1b is the spectrum of the same oil spiked with 0.5% *trans,trans*-2,4-decadienal. In this spectrum it is difficult to detect the presence of this contaminant by simple inspection. Upon ratioing the spectrum of the spiked sample against that of the unspiked oil (Fig. 1c), the spectral features of decadienal became quite apparent (bands in the regions 1750–1600 and 1200–900 cm^{-1} as well as two weak bands in the 2850–2700 cm^{-1} region), as the spectral contributions of the oil have been ratioed out, leaving a clear spectral window that allows the differences between the two oil samples to be detected.

The ratio technique is a sensitive means of detecting relative spectral changes as long as the signal reaching the detector is strong enough to be measured accurately. For example, for regions of intense absorption in Figure 1a (i.e., the triglyceride ester linkage and major CH bands, where absorbance values are >2.0 absorbance units), the signal reaching the detector is too small to be sampled properly, leading to digitization noise in the ratioed spectrum as seen in Figure 1c at ≈3000–2800 and ≈1750 cm^{-1}. This problem can be avoided by reducing the effective path length of the cell so that such bands are not as intense, and will ratio out, but at the expense of sensitivity in other regions. This is illustrated by comparing Figures 1c and 1d, the ratioed spectra obtained for the same spiked sample on a 40 and a 45° ZnSe crystal, respectively, the latter having a lower depth of penetration and, hence, a shorter effective path length. In Figure 1d, negative peaks are observed in the CH stretching region and at the position of the triglyceride ester linkage absorption, whereas digitization noise is observed in these regions in Figure 1c. These negative peaks arise because of the dilution effect produced by spiking, such that the oil absorptions are more intense in the spectrum of the unspiked oil than in that of the spiked sample. Because of the lower depth of penetration of the 45° crystal, the spectral features of *trans,trans*-2,4-decadienal are clearly much weaker in Figure 1d than in Figure 1c, with the weak bands in the 2850–2700 cm^{-1} region not discernible. In general, unless measurements are specifically required in regions of high absorption, it is best to use a longer path length and benefit from the resulting increased sensitivity. The ability to routinely carry out spectral ratioing (single-beam spectra) and/or its equivalent (spectral subtraction) in the case of absorbance spectra in an accurate and reproducible manner is a key element in our approach to developing FTIR-based methods for oil analysis.

Analysis of oxidative reference compounds. A spectral library was prepared of compounds having functional groups representative of common oil oxidation products. Alcohols, saturated aldehydes and α,β-unsaturated aldehydes, which have been reported as major secondary oxidation products (2,4), were all represented in the spectral library by C_6 homologues, with $\alpha,\beta,\gamma,\delta$-unsaturated aldehydes represented by *trans,trans*-2,4-decadienal, a major decomposition product from heated oxidized linoleate (4). *t*-Butyl hydroperoxide was selected to represent hydroperoxides because of its stability. Although ketones are minor products in oxidized oils, a C_6 allylic ketone was included in the spectral library to investigate the extent of overlap between the aldehyde and ketone absorptions. Oleic acid and water were also included in view of their possible presence in oils, particularly under hydrolysis conditions. While the literature abounds with spectral assignments for compounds of all these types (18,19), it was necessary to obtain basic spectral data for these compounds in oil to account for any spectral shifts that might occur in this medium (e.g., as a result of hydrogen bonding). Table 1 tabulates the functional group frequencies determined by an analysis of these reference spectra and gives their relative absorptivities in relation to the strongest absorbing functional group (ν C=O of hexenal = 1.0).

TABLE 1

Peak Positions and Relative Strengths of the Functional Group Absorptions of Reference Compounds Representative of Products Formed in Oxidized Oils[a]

Compound	Vibration	Peak maximum	Relative absorptivity[c,d]
Water	ν ***OH***	3650 and 3550 cm^{-1}	NA
Water	δ ***HOH***	1625 cm^{-1}	NA
Hexanol	ν R***OH***	3569 cm^{-1}	0.06
t-Butyl hydroperoxide	ν R***OOH***	3447 cm^{-1}	0.04
Hexanal	ν R***HC***=O	2810 and 2712 cm^{-1}	0.02 and 0.03
Hexanal	ν RH***C***=***O***	1727 cm^{-1}	0.20
Hexenal[b]	ν R***HC***=O	2805 and 2725 cm^{-1}	0.03 and 0.03
Hexenal	ν RH***C***=***O***	1697 cm^{-1}	1.00
Hexenal	ν R***C***=***C***H-HC=O	1640 cm^{-1}	0.10
Hexenal	δ R***C***=***C***H-HC=O	974 cm^{-1}	0.25
2,4-Decadienal[b]	ν R***HC***=O	2805 and 2734 cm^{-1}	0.03 and 0.02
2,4-Decadienal	ν RH***C***=***O***	1689 cm^{-1}	0.81
2,4-Decadienal	ν R***C***=***C***H-HC=O	1642 cm^{-1}	0.52
2,4-Decadienal	δ R***C***=***C******H***-HC=O	987 cm^{-1}	0.27
4-Hexen-3-one[b]	ν R***C***(=***O***)HC=CHR	1703 and 1679 cm^{-1}	0.23 and 0.38
4-Hexen-3-one	ν RC(=O)H***C***=***C***HR	1635 cm^{-1}	0.32
4-Hexen-3-one	δ RC(=O)H***C***=***C******H***-R	972 cm^{-1}	0.29
Oleic acid	ν RCO***OH***	3310 cm^{-1}	0.03
Oleic acid	ν R***C***(=***O***)OH	1711 cm^{-1}	0.25

[a]The bonds of each functional group that are responsible for the absorption band(s) are presented in bold/italic type.
[b]All double bonds in the *trans* form; [c]Relative to a value of 1 for the strongest absorption band.
[d]Values are for spectra recorded in the attenuated total reflectance mode.

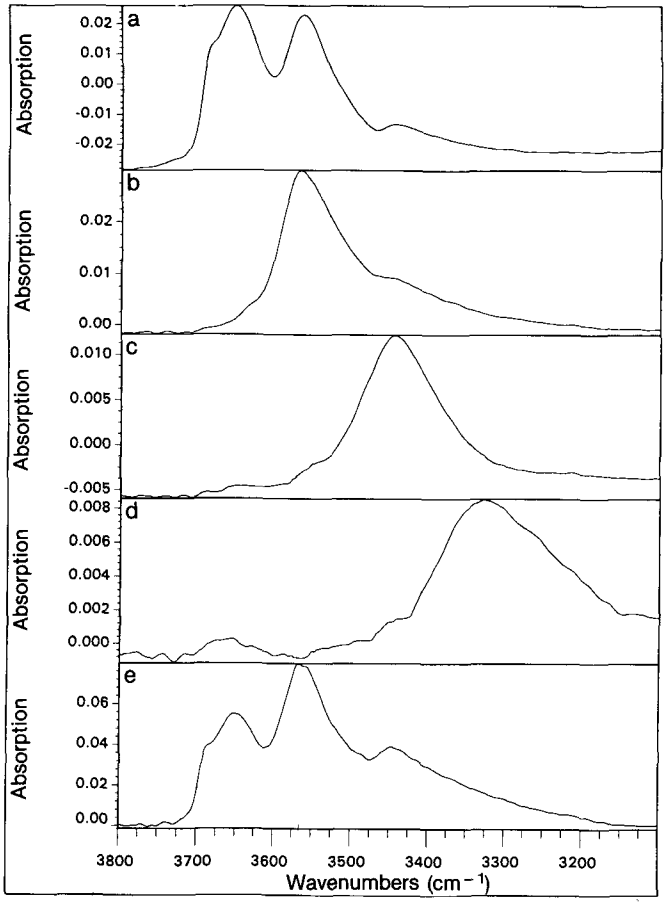

FIG. 2. The OH stretching region (3800–3100 cm^{-1}) in the attenuated total reflectance/Fourier transform infrared spectra of oxidation reference compounds obtained by ratioing the single-beam spectra of olive oil spiked with the reference compound against the single-beam spectrum of pure olive oil: (a) H_2O; (b) hexanol; (c) *t*-butyl hydroperoxide; (d) oleic acid; (e) spectrum obtained by co-adding spectra a–d. All reference compounds were added at 2% (w/w), except for H_2O, which was added to saturation levels.

Table 1 shows that each of the various types of oxidation products gives rise to discernible and characteristic absorptions in the FTIR spectrum. Some comments are warranted with respect to the positions of these absorptions. Figure 2 presents the OH stretching region in the water, *t*-butyl hydroperoxide, hexanol and oleic acid reference spectra, plus the composite spectrum obtained by co-adding these spectra. Figure 2a–d illustrates that the hydroxyl absorptions of all these compounds occur in the same vicinity (3800–3100 cm^{-1}) and are inherently broad due to hydrogen bonding. Figure 2e, the composite spectrum, illustrates the extensive overlap that occurs if all these compounds are present simultaneously in equal amounts. Even with this overlap, most peaks, except for the hexanol band and the lower frequency component of the water band, appear to be sufficiently separated to enable identification. The presence of alcohol can be established by comparing the intensity of the water/alcohol overlapping band to that of the higher frequency component of the water band and/or the other characteristic absorption of water at 1625 cm^{-1} (not shown).

Figure 3 illustrates the carbonyl region in the hexanal, hexenal, decadienal, hexenone and oleic acid reference spectra, plus their composite spectrum. The aldehydes all exhibit C=O stretching bands in the 1730–1680 cm^{-1} region, as shown in Figure 3a–c, as well as weaker CH stretching bands between 2820 and 2700 cm^{-1} (not shown). The presence of α,β unsaturation causes a substantial shift of the C=O stretching band to lower wavenumbers (from 1727 cm^{-1} for hexanal to 1697 cm^{-1} for *trans*-2-hexenal), which is accentuated by the presence of an additional conjugated double bond (1689 cm^{-1} for *trans, trans*-2,4-decadienal). The α,β-unsaturated aldehydes can also be distinguished by their C=C stretching absorption at ≈1640 cm^{-1}, which exhibits exceptional intensity due to conjugation with the aldehyde group, and their bands in the *trans* C=CH bending region. In the latter region (not shown), *trans,trans*-2,4 decadienal exhibits an

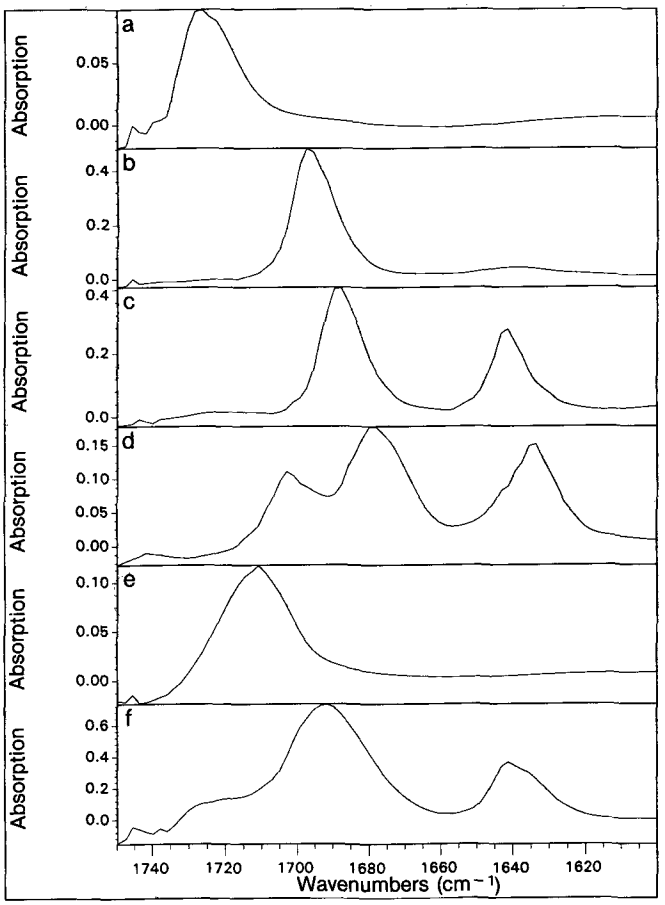

FIG. 3. The carbonyl region (1750–1600 cm^{-1}) in the attenuated total reflectance/Fourier transform infrared spectra of oxidation reference compounds obtained by ratioing the single-beam spectra of olive oil spiked with the reference compound against the single-beam spectrum of pure olive oil: (a) hexanal; (b) *trans*-2-hexenal; (c) *trans, trans*-2,4-decadienal; (d) *trans*-4-hexen-3-one; (e) oleic acid; (f) spectrum obtained by co-adding spectra a–e. All reference compounds were added at 2% (w/w).

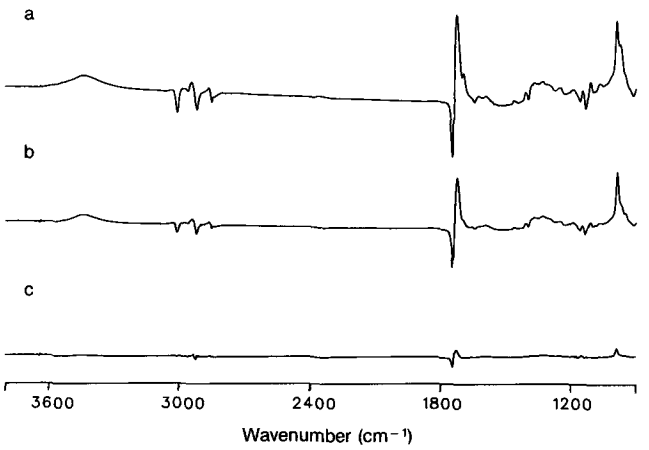

FIG. 4. Attenuated total reflectance/Fourier transform infrared spectra of safflower oil heated to 76°C on the surface of a 45° ZnSe ATR crystal: (a) t = 16 h; (b) t = 8 h; (c) t = 1 h. The spectra have been ratioed against the spectrum recorded at t = 0.

additional characteristic absorption at 987 cm^{-1} due to the conjugated *trans* double bonds, whereas *trans*-2-hexenal absorbs at 974 cm^{-1}, characteristic of the isolated *trans* double bond. On the basis of the characteristic spectral features of these reference aldehyde compounds, it should be possible to distinguish in general between saturated, α,β-unsaturated and $\alpha,\beta,\gamma,\delta$-unsaturated aldehydes.

Figure 3d illustrates the spectrum of *trans*-4-hexen-3-one, an allylic ketone. The C=O stretching absorption is a doublet with one component, corresponding to the *s-cis* isomer (19), appearing where saturated ketones normally absorb, while the second absorption, corresponding to the *s-trans* isomer, is in close proximity to the C=O stretching absorption of *trans,trans*-2,4-decadienal. It also exhibits C=C stretching and *trans* C=C-H bending absorptions that overlap with the corresponding bands of *trans*-2-hexenal. Thus, it would be difficult to distinguish either saturated or unsaturated ketones from α,β-unsaturated aldehydes in an oxidized oil, especially as these compounds are generally present in trace amounts. Aldehydes, however, can be definitively distinguished from ketones on the basis of their characteristic CH stretching absorptions in the 2820–2700 cm^{-1} region.

The last major functional group of interest is the carboxyl group of FFAs, represented by oleic acid, which absorbs at 1711 cm^{-1} (Fig. 3e), as well as in the OH stretching region, as discussed earlier. The carboxyl group produces a clean, single band in the C=O stretching region; however, as shown in the co-added spectrum (Fig. 3f), this absorption lies between two aldehyde bands (hexanal and *trans*-2-hexenal) and would be difficult to distinguish in the spectrum of an oxidized oil unless FFAs are present in relatively large amounts.

Overall, based on the co-added spectra in the hydroxyl, carbonyl and *trans* double bond regions (not shown), the indications are that substantial spectral information should be available if products of the types represented by the reference compounds are formed during the oxidative process. To acertain whether this expectation is met in real systems undergoing oxidation, a variety of oils were oxidized under accelerated conditions and followed spectrally as a function of time. Examples of the results from these experiments are presented below to illustrate the types of spectral changes observed in oils undergoing oxidation.

Moderate heating—safflower oil. To simulate moderate but accelerated oxidative conditions, safflower oil was placed on a heated (75°C) horizontal ATR accessory. The combination of temperature and the large surface area of the oil that is exposed to air speeds up the autoxidative process. As such, the system simulates the active oxygen method (AOM), except that oxidative changes can be monitored in real time as oxidation proceeds. Figure 4 illustrates the spectra recorded at t = 1, 8 and 16 h, ratioed against the spectrum recorded at t = 0. These spectra were acquired on a 45° ZnSe crystal to minimize digitization noise in regions of intense oil absorptions. As oxidation progresses with time, one can readily see, from left to right in Figure 4: (i) the appearance of a broad band in the OH stretching region (3800–3200 cm^{-1}), (ii) a decrease in the CH stretching vibrations (3050–2800 cm^{-1}), (iii) a large decrease in the triglyceride ester linkage absorption (1744 cm^{-1}), (iv) the appearance of

peaks on the low frequency side of the triglyceride ester linkage absorption and (v) a sharp rise in peaks in the *trans* double bond region (1000–900 cm^{-1}). All positive bands in Figure 4 are an unambiguous indication of the production of new molecular species. However, negative bands do not necessarily represent the loss of functional groups. For example, the sharp decrease in the triglyceride ester linkage absorption could be taken to imply that an extensive amount of hydrolysis has taken place; however, not only is this unlikely under these moderate conditions, it definitely does not occur, as there is no spectral evidence of concurrent FFA formation. In fact, the decrease in the ester linkage absorption (and in some of the CH absorptions) is caused by oxygen being chemically incorporated into the oil as oxidation products are formed. This oxygen uptake, in effect, dilutes the sample relative to the reference, and, as a consequence, bands that are common to the sample and the reference oil do not ratio out perfectly, but instead exhibit negative intensity in the ratioed spectrum. For each absorption band of the oil, the negative band intensity in the ratioed spectrum due to this oxygen uptake effect is proportional to its intensity in the oil's absorbance spectrum (i.e., its spectrum ratioed against air), and thus the greatest effects are observed for the strongest absorption bands, such as the triglyceride ester linkage absorption. One can determine whether a negative band is due solely to the oxygen uptake effect or to a combination of this effect and the actual loss of a functional group by comparing its intensity to that of a strong reference band associated with a stable and relatively unreactive functional group. The absorption band of the triglyceride ester linkage, which is one of the more stable bonds in an oil system unless thermally stressed (>200°C), can serve as such a reference band, provided that the path length of the IR cell is sufficiently narrow to avoid digitization noise on ratioing this band (e.g., 45° ZnSe ATR). Under these conditions, dividing the peak height of the (negative) ester linkage band in the ratioed spectrum, obtained at t = x h, by the height of this band in the absorbance spectrum (i.e., ratioed against air; Fig. 1a), recorded at t = 0, provides a measure of the dilution of the sample due to the oxygen uptake effect:

$$\% \text{ dilution } (t = x \text{ h}) = \% \text{ decrease in peak height @ } 1744 \text{ cm}^{-1} = (|A_{1744}{}^{r}{}_{(t = x \text{ h})}|/A_{1744(t = 0)}) \times 100 \quad [2]$$

where $A_{1744}{}^{r}$ and A_{1744} are the peak heights of the triglyceride ester linkage absorption in the ratioed spectrum at t = x h and the absorbance spectrum at t = 0, respectively. As the extent of dilution is proportional to the amount of oxygen taken up by the sample, this measure is, in effect, an indicator of the overall extent of oxidation. The percent decrease in peak height that any other negative band represents can be calculated in the same manner $[|A_{\nu}{}^{r}{}_{(t = x \text{ h})}|/A_{\nu(t = 0)}) \times 100]$ and compared to the value obtained for the ester linkage band (see inset in Fig. 5). A definitive difference in these values is indicative that changes beyond the oxygen uptake effect contribute to the negative band intensity.

With these considerations in mind, it is useful to examine each of the major spectral regions in some detail (see i–iii).

(i) OH region. Figure 5 shows a detailed view of the 3800–2800 cm^{-1} region for the same experiment as in Figure 4. The broad peak centered at 3444 cm^{-1} is the O-H stretching vibration of hydroperoxides, a peak assignment established by early work on the oxidation of methyl linoleate (15). There is no indication of alcohol being formed as the peak remains symmetrical throughout the experiment, as judged by measuring the intensities at points 100 cm^{-1} on either side of the maximum, nor is there any evidence of water or FFA formation. The progressive increase in the hydroperoxide band with time is accompanied by a decrease in the peak at 3011 cm^{-1}, assigned to the C-H stretching vibration of *cis* double bonds. This represents a net loss of *cis* double bonds as opposed to an oxygen uptake effect, as seen by the much greater percent decrease in this band relative to the triglyceride ester linkage band (Fig. 5, inset). The negative band at 2922 cm^{-1} (Fig. 5), assigned to the CH_2 stretching vibration, although comparable in magnitude to the *cis* band, can be largely attributed to an oxygen uptake effect, given that this band is an order of magnitude stronger than the *cis* band in the absorbance spectrum (see Fig. 1a). Hence, Figure 5 clearly indicates that there is significant formation of hydroperoxides coupled with a concomitant loss of *cis* double bonds, a well-known characteristic of lipids undergoing oxidation under moderate conditions (2).

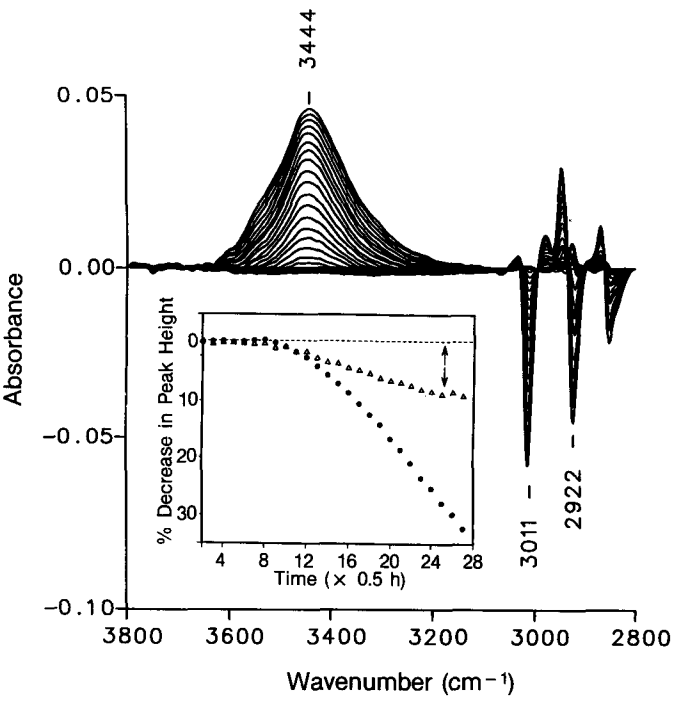

FIG. 5. Spectral overlay plot illustrating changes in the 3800–2800 cm^{-1} region of the attenuated total reflectance (ATR)/Fourier transform infrared spectrum of safflower oil heated to 76°C on the surface of a 45° ZnSe ATR crystal as a function of time. The overlaid spectra were recorded at 30-min intervals and have been ratioed against the spectrum recorded at t = 0. Inset: Percent decrease in the peak heights of the *cis*-C=CH stretching (●) and triglyceride ester linkage (△) bands vs. time. The arrow indicates the magnitude of the dilution of the oil due to the oxygen uptake effect.

(ii) Carbonyl region. Figure 6 illustrates the changes taking place in the carbonyl region (1750–1650 cm^{-1}), excluding the triglyceride ester linkage band discussed

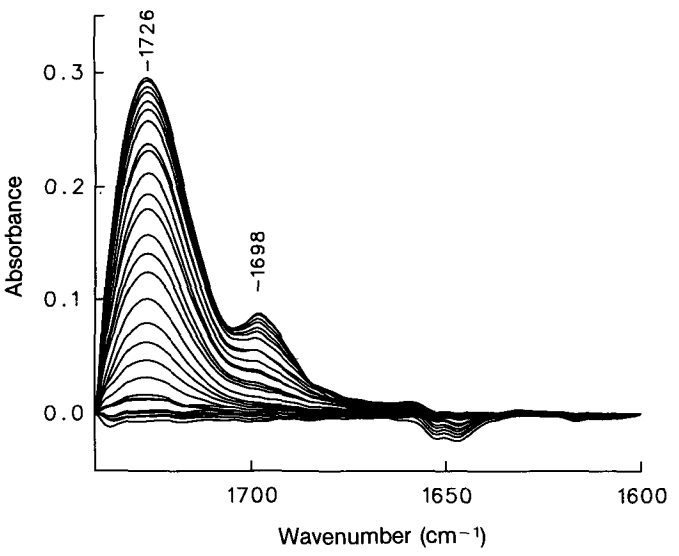

FIG. 6. Spectral overlay plot illustrating changes in the 1750–1600 cm^{-1} region of the ATR/Fourier transform infrared spectrum of safflower oil heated to 76°C on the surface of a ZnSe ATR crystal as a function of time. The overlaid spectra were recorded at 30-min intervals and have been ratioed against the spectrum recorded at t = 0. See Figure 5 for abbreviation.

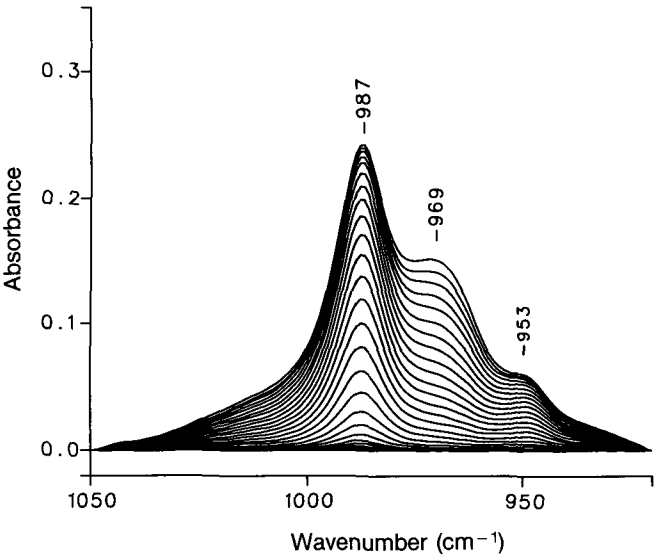

FIG. 7. Spectral overlay plot illustrating changes in the 1050–900 cm^{-1} region of the ATR/Fourier transform infrared spectrum of safflower oil heated to 76°C on the surface of a ZnSe ATR crystal as a function of time. The overlaid spectra were recorded at 30-min intervals and have been ratioed against the spectrum recorded at t = 0. See Figure 5 for abbreviation.

earlier. The most significant change is the appearance of two bands at 1726 and 1698 cm^{-1} with these positions being almost identical to those associated with the characteristic absorptions seen for hexanal and 2-hexenal in olive oil, respectively (Fig. 3a and b), and it is likely that these peaks are representative of saturated and α,β-unsaturated aldehydes. There is no indication in these spectra that any FFAs are formed under these conditions, as there is no overt absorption band at 1711 cm^{-1}. As noted in our discussion of the library reference spectra, the identification of ketones in the presence of aldehydes is difficult, so it is not possible to determine from Figure 6 whether ketones are being produced. Within the region shown in Figure 6, there is a small negative band centered at 1650 cm^{-1}, which is due to the C=C stretching absorption of unsaturated fatty acids in the triglycerides. A plot of the type shown in Figure 5 showed that the negative intensity of this band is not solely due to an oxygen uptake effect but can be attributed to a net loss of C=C bonds. However, changes in the C=C stretching absorption in the spectra of oxidized oils would generally be difficult to interpret because of the shifts in position and large differences in the extinction coefficient of this absorption for *cis* and *trans* double bonds and for double bonds conjugated with carbonyl groups, such as are commonly found in products of oxidative breakdown of oils.

(iii) trans *Double bond region.* Major changes take place, as oxidation proceeds, in the region between 1000 and 900 cm^{-1} (Fig. 7), where the C=C-H bending vibrations of *trans* double bonds occur. The appearance of two bands at 987 and 953 cm^{-1}, in approximately a ≈2:1 ratio, is apparent in the early stages of oxidation, while later on, the band at 987 cm^{-1} exhibits a slight shift toward higher wavenumbers and a shoulder on this band, at 969 cm^{-1}, becomes apparent. This region has been extensively investigated in the spectra of hydroperoxides formed and isolated from methyl linoleate undergoing oxidation (16), with the peaks observed at 982 and 948 cm^{-1} (in CS_2 solution) assigned to *cis,trans*-conjugated dienes. In the spectrum of a mixture of *trans,trans* and *cis,trans* conjugated dienes, a shift of the 982 cm^{-1} band to 985 cm^{-1} was observed, whereas the pure *trans,trans*-conjugated diene exhibits a single band at 988 cm^{-1}. Taking into account the slight shifts in peak positions on going from CS_2 solution to neat oil, Figure 7 demonstrates the formation of conjugated dienes, with the amount of *trans, trans* conjugated dienes relative to *cis,trans* conjugated dienes increasing as a function of time, as well as the formation of isolated *trans* bonds, indicated by their characteristic absorption at 969 cm^{-1}.

Real-time oxidation plots. Based on the results shown in Figures 4–7, it is possible, by using the FTIR ratio method, to follow the appearance or disappearance of the major functional groups in an oil as a function of time as oxidation proceeds. To obtain a graphical representation of the relative changes in the functional group absorptions during the course of oxidation, the spectrometer was programmed to measure the absorbance values (peak heights) at the wavenumbers listed in Table 1 for the peak maxima of the functional group absorptions at specified time intervals during oil oxidation experiments. The values at each wavelength measured were subsequently normalized with respect to the maximum absorbance value reached at that wavelength (A_ν/A_ν^{max}) during the course of the experiment and plotted against time to produce a plot that represents the course of the oxidation process (real-time oxidation plot).

(i) Oxidation at moderate temperatures—safflower/cottonseed oil. Figure 8 is a real-time oxidation plot for the initial stages (15 h at 76°C) of autoxidation of safflower oil, showing the relative changes in the hydroperoxide, aldehydes *cis* and *trans* absorbances as a function of time.

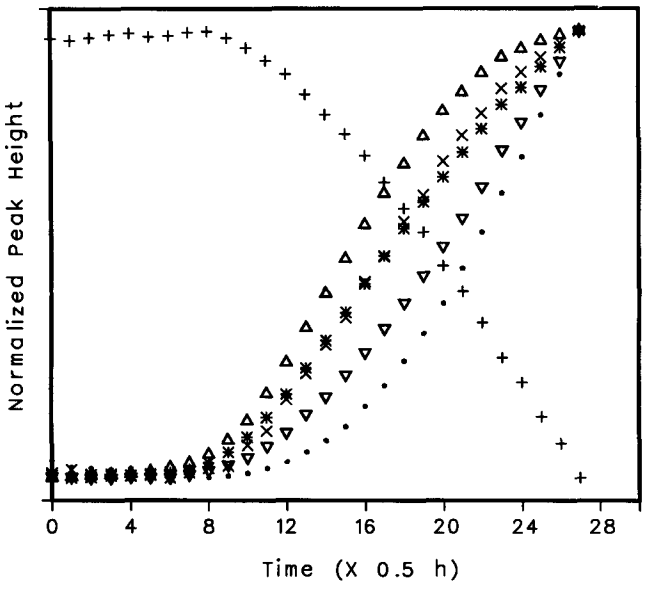

FIG. 8. Real-time oxidation plot for safflower oil at 76°C, showing the normalized peak heights of the major functional group absorption bands vs. heating time; +, *cis* C=CH stretching absorption (3011 cm^{-1}); △, *trans* C=C-H conjugated (987 cm^{-1}); x, ROOH (3444 cm^{-1}); *, R′CH_2CHO (1726 cm^{-1}); ▽, *trans* C=CH isolated (969 cm^{-1}); ●, R″C=C-CHO (1698 cm^{-1}).

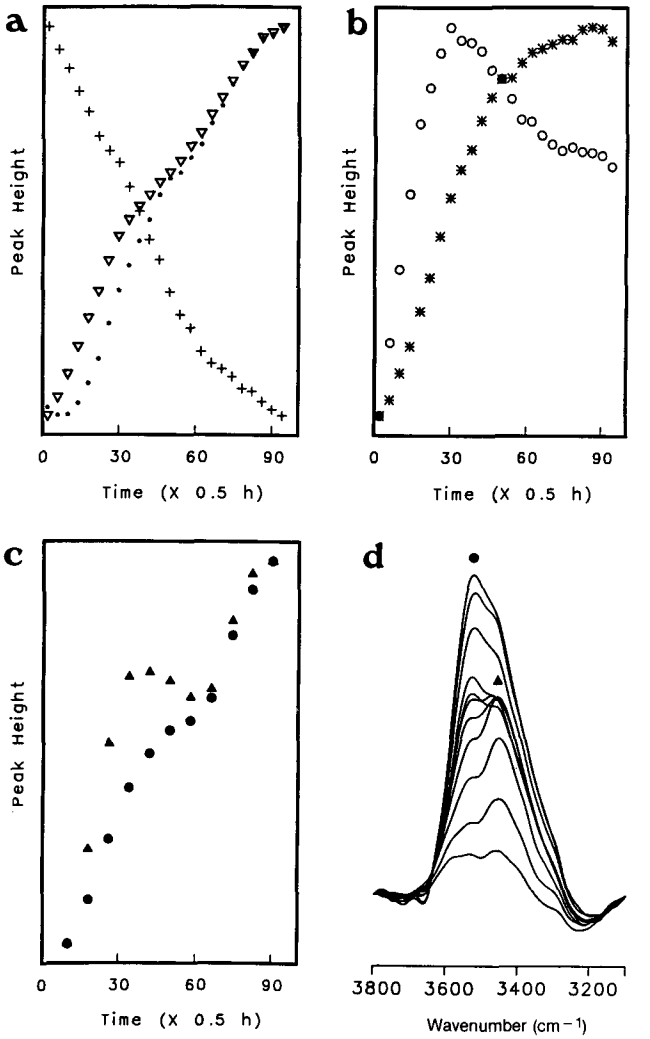

FIG. 9. Partitioned real-time oxidation plot for cottonseed oil at 76°C: (a) +, *cis* C=CH stretching absorption (3011 cm^{-1}); ▽, R′CH_2CHO (1726 cm^{-1}); ●, R″C=C-CHO (1698 cm^{-1}); (b) ○, *trans* C=CH conjugated (987 cm^{-1}); *, *trans* C=CH isolated (969 cm^{-1}); (c) ▲, ROOH (3444 cm^{-1}); ●, R′OH (3544 cm^{-1}); (d) overlaid spectra in the OH stretching region, illustrating the overlap of the ROOH and R′OH bands.

As such, it clearly shows that after an initial period of stability (induction period), there is a loss of *cis* double bonds with a concomitant appearance of hydroperoxides, aldehydes and *trans* double bonds. No alcohols or FFAs were in evidence in this experiment. In contrast, in a subsequent experiment on cottonseed oil, oxidized at the same temperature but for a longer period of time (50 h), a more complicated real-time oxidation plot is obtained, which has been separated into three frames for clarity (Fig. 9a-c). Once again, there is a rapid depletion of *cis* double bonds and the production of aldehydes (Fig. 9a), with α,β-unsaturated aldehydes being the last to appear. Figure 9b illustrates the *trans,trans* and *cis,trans* conjugated dienes rising steadily, reaching a maximum, and subsequently beginning to decrease, while the band due to isolated *trans* bonds rises rapidly and then begins to plateau. Figure 9c illustrates that both hydroperoxides and alcohols are being formed in this system, showing an initial rise up to 20 h, followed by a drop and plateau, respectively, subsequently followed by a rise in the relative absorbance values of both products. A closer examination of this region of the spectrum (Fig. 9d) indicates that, in actual fact, hydroperoxides (▲) are produced initially, maximize and then start to decrease; however, the absorbance values measured for the hydroperoxide band continue to rise due to overlap with the continually rising alcohol band (●). The inflection point at ≈30 h in the alcohol plot is also an anomaly due to the alcohol band being pulled down by the decrease in the overlapping hydroperoxide band. Referring back to Figure 9b, a similar effect causes the plateau in the isolated *trans* plot, the band being dragged down by the concurrent drop in the *cis, trans/trans,trans* double bond signal, due to the close proximity of these two bands. When spectral subtractions were carried out to compensate for these overlaps, both the hydroperoxide and the conjugated diene absorptions in fact dropped to negligible values by the end of the experiment. Thus, although real-time oxidation plots provide an excellent overview of the chemical changes taking place as oils oxidize, some caution is required in interpreting them in absolute terms, especially in the case of hydroperoxides.

(ii) Thermally stressed oil—safflower. To study the oxidation behavior of oils under various degrees of thermal stress, FTIR spectra were recorded in the transmission mode, the oil being heated and oxidized in a reservoir and cycled continuously through a transmission flow cell. Safflower oil was heated to 100, 130 and 230°C for 40, 160 and 200 min, respectively, with spectra recorded every 20 min. Figure 10 illustrates spectra recorded at the end of each heating stage over the three main spectral regions. Looking at the OH stretching region, only hydroperoxides are present after 40 min at 100°C, while after 160 min

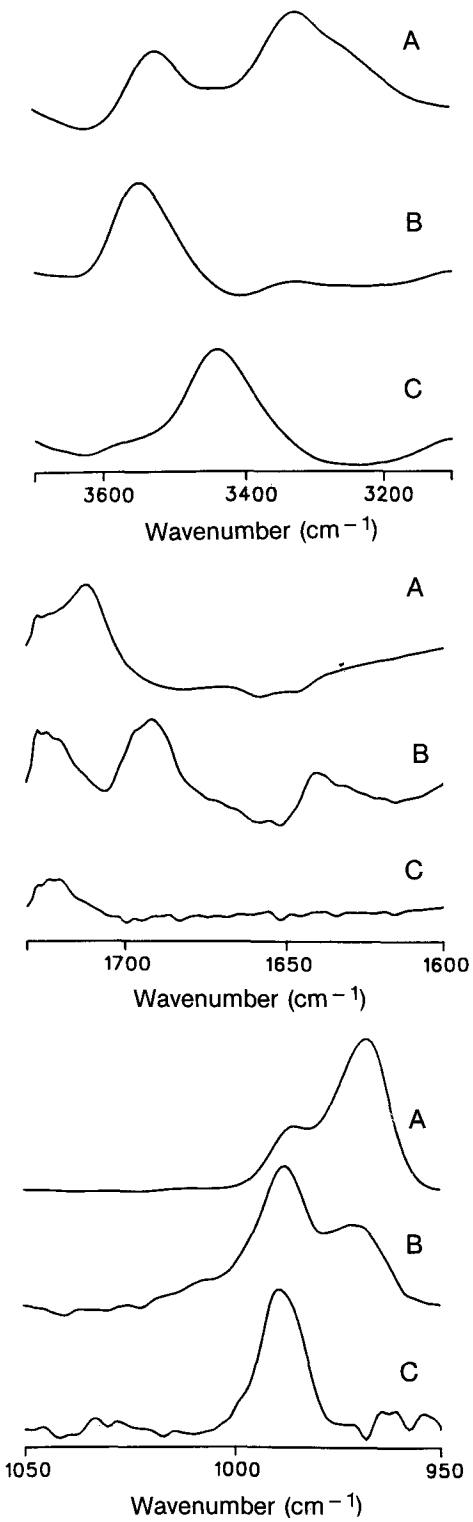

FIG. 10. The Fourier transform infrared spectra in the OH stretching, (3700–3100 cm^{-1}), carbonyl (1750–1600 cm^{-1}) and *trans* double bond regions (1050–950 cm^{-1}) of thermally stressed safflower oil, obtained by ratioing the single-beam spectrum recorded after 200 min at 230°C (A), 160 min at 130°C (B), and 40 min at 100°C (C) against that recorded at the beginning of the experiment.

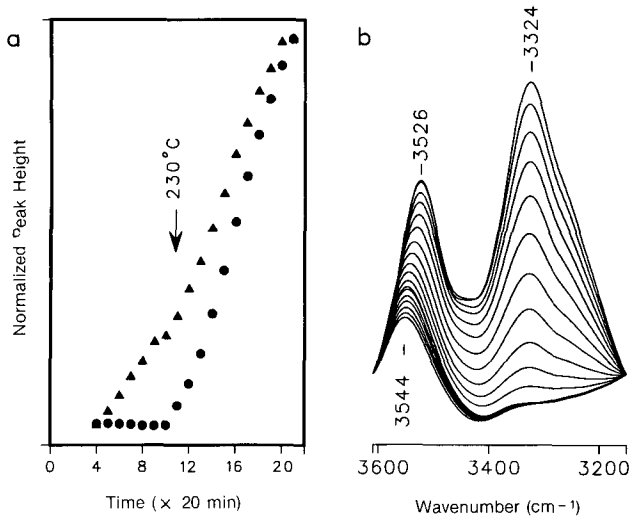

FIG. 11. (a) Partial real-time oxidation plot for the RO-H (▲, 3544 cm^{-1}) and R′C(=O)O-H (●, 3324 cm^{-1}) stretching absorptions for safflower oil heated from 130 to 230°C and then maintained at 230°C for 200 min; (b) corresponding overlaid spectra, illustrating the shift in the OH stretching absorption maximum from 3544 to 3526 cm^{-1} as the temperature is increased.

at 130°C, the hydroperoxides have disappeared and alcohols have formed. Under extreme thermal stress (230°C for 200 min), there is an extensive formation of FFAs, as indicated by the appearance of a band at 3324 cm^{-1} (OH stretching band of the carboxyl group), as well as alcohols; however, the alcohol band appears to have shifted slightly. In the carbonyl region, at 100°C, a small amount of unsaturated aldehydes is evident, while at 130°C α,β-unsaturated aldehydes have formed in significant amounts, and saturated aldehydes have increased further. At 230°C, the predominant band in this region is at 1711 cm^{-1} due to the formation of FFAs, with some saturated aldehydes remaining, but α,β-unsaturated aldehydes have disappeared completely. The spectra in the *trans* double bond region illustrate the initial formation of *cis,trans* and *trans,trans* conjugated dienes at 100°C, followed by the progressive conversion of the conjugated bonds to isolated *trans* bonds on going to 130 and 230°C. A real-time oxidation plot is presented for only the alcohols and the FFAs in Figure 11a. Raising the temperature to 230°C initiates thermal hydrolysis as evidenced by the rapid increase in FFAs. There is a concurrent slope change in the alcohol plot, just as the FFAs begin to be released. Figure 11b illustrates the detailed spectral changes associated with the real-time oxidation plot (Fig. 11a) There is a band shift in the alcohol region coinciding with the appearance of FFAs. Interpreting these spectra, there is a shift from the production of alcohols from hydroperoxide breakdown (3544 cm^{-1}) to the appearance of alcohol functional groups associated with mono- and diglycerides (3526 cm^{-1}), produced when FFAs are liberated. Although this is a minor spectral change, it demonstrates that one can even differentiate between different types of alcohols in the spectra of oxidized oils.

Although the oxidation conditions and oils studied here are not all-inclusive, they were adequate to produce most of the compounds commonly associated with lipid oxidation and serve to illustrate the information obtainable by

FTIR spectroscopy in monitoring oil oxidation. Practical applications based on this approach can be envisaged, e.g., real-time monitoring of oil on a heated ATR crystal being utilized as a modified AOM or use of a flow cell system for on-line monitoring of frying oils.

Quantitative aspects. Based on the results obtained from this limited spectroscopic survey of changes taking place in oils undergoing oxidation, it is clear that relative changes can be readily measured, although there are some problems in interpreting such changes in the case of overlapping bands (e.g., alcohol and hydroperoxide absorptions). Generally, the key products of interest in assessing the oxidative status of oils are hydroperoxides, alcohols and aldehydes, with FFAs becoming important in high-temperature stressed oils. Judging from our spectral study, FTIR spectroscopy could be further developed into a relatively simple technique for the quantitative determination of common oxidation products in oils. We have already developed a quantitative method for the determination of FFAs in oils based on the ratio concept presented in this paper (13); however, a number of considerations require elaboration for the further development of a generalized method of quantitation, as outlined below.

(i) Obtaining a reference oil. A crucial consideration in making use of the ratio method is that one should have a high degree of confidence that the reference oil is free of oxidative contaminants. If a compound to be analyzed for, or some other contaminant absorbing at the frequency used for its measurement, is present in the reference oil, the absorption band of this compound in the ratioed spectrum of the sample will be reduced in intensity to the extent that the contaminant is present in the reference oil. As such, one would detect changes relative to the reference oil, but would not obtain an accurate concentration value. This is not a problem if one is confident that the reference oil is "fresh"; however, it is best to ensure a zero baseline by cleaning up the reference oil. A simple procedure is to pass the oil through activated silica gel, which removes all compounds with any degree of polarity (water, alcohols, hydroperoxides, aldehydes, FFAs, etc.). The efficacy of this procedure was assessed spectrally and confirmed by PV, AV and FFA determinations. To determine spectroscopically that alcohols, FFAs and hydroperoxides were completely removed, the spectrum of the purified oil was ratioed against that of a fraction of this oil that had been treated with D_2O. This treatment converts all OH functional groups to OD functional groups, which absorb at a lower frequency due to their higher mass, and thus ratioing against the D_2O-treated sample provides a clear window in the OH stretching region. No OH bands were observed in the spectra of the silica gel-treated samples, indicating that alcohols, FFAs and hydroperoxides were completely removed. Hence, the silica gel treatment provides a simple means of obtaining a "clean" reference oil.

(ii) Oxidation calibration standards. With the availability of a "clean" reference oil, it is possible to prepare calibration standards by spiking this oil with compounds that are spectroscopically representative of the major oxidation products, e.g., *t*-butyl hydroperoxide, hexanol, hexanal, *trans*-2-hexenal and *trans,trans*-2,4-decadienal. This approach is both simple and practical and expresses the absorbance values of oil samples in terms of the equimolar concentrations of the reference compounds. In formulating a quantitative approach of this nature, one has to consider the potential interferences due to the overlap of water, hydroperoxide and alcohol absorptions in the OH region and the extensive overlap of bands in the carbonyl region. These interferences can be accounted for by preparing a set of standards containing randomized quantities of the reference compounds in a clean oil and carrying out multivariate analysis, which provides cross corrections for the overlapping bands. A number of mathematical approaches are available, the simplest being multiple regression based on peak height measurements. Alternatively, FTIR chemometric packages, based on **P**- or **K**-matrix (20,21) or partial least squares methods (22), may be employed. Such software works directly with spectral data and can typically abstract absorbance values and/or integrated intensities from the spectra, calculate the calibration factors, and print out the concentrations of unknowns. Once a calibration is achieved, it would be useful to express the oxidative state of an oil in terms of % *t*-butyl hydroperoxide, % hexanol, and, by summing all the aldehyde and ketone contributions, % total carbonyls. Alternatively, similar techniques could be used to relate selected absorptions to well-known chemical measures of oxidation, e.g., PV and AV. Either approach would take some effort to develop; however, once this is done, the spectroscopic and mathematical elements could be preprogrammed into the spectrometer, resulting in a method that would be simple and directly applicable to the quality control of oils, but requiring no spectroscopic knowledge to carry out an analysis.

This study demonstrates the power and utility of FTIR spectroscopy in following and determining the relative state of oxidation of an oil under a variety of conditions. The capability to assess the relative oxidative state of an oil sample or to monitor oil oxidative processes by FTIR spectroscopy in real time appears to be workable and should be especially useful to the general quality control of edible oils. The next challenge will be to develop, program and assess the quantitative approaches suggested and establish whether concurrence between FTIR spectral changes and conventional chemical methods can be obtained, so that the FTIR results can be expressed in analytical terms with which the edible oil industry is familiar.

ACKNOWLEDGMENTS

The authors thank the Natural Sciences and Engineering Research Council of Canada for funding this research, Nicolet Instrument for providing the 8210 spectrometer and E. Despland for technical assistance.

REFERENCES

1. Paquette, G., D.B. Kupranycz and F.R. van de Voort, *Can. Inst. Food Sci. Technol. J. 18*:112 (1985).
2. Paquette, G., D.B. Kupranycz and F.R. van de Voort, *Ibid. 18*:197 (1985).
3. Frankel, E., *Prog. Lipid Res. 19*:1 (1980).
4. Frankel, E., *Ibid. 22*:1 (1982).
5. Frankel, E., *Ibid. 23*:197 (1985).
6. *Official Methods and Recommended Practices of the American Oil Chemists' Society*, 4th edn., American Oil Chemists' Society, Champaign, 1989.
7. van de Voort, F.R., and A.A. Ismail, *Trends Food Sci. Technol. 2*:13 (1991).
8. van de Voort, F.R., *Food Res. Int. 25*:397 (1992).

9. van de Voort, F.R., J. Sedman, G. Emo and A.A. Ismail, *J. Assoc. Off. Anal. Chem. 75*:780 (1992).
10. van de Voort, F.R., J. Sedman, G. Emo and A.A. Ismail, *Food Res. Int. 25*:193 (1992).
11. van de Voort, F.R., J. Sedman and A.A. Ismail, *Food Chemistry 48*:213 (1993).
12. van de Voort, F.R., J. Sedman, G. Emo and A.A. Ismail, *J. Am. Oil Chem. Soc. 69*:1118 (1992).
13. Ismail, A.A., F.R. van de Voort, G. Emo and J. Sedman *Ibid. 70*:335 (993).
14. Steiner, J., *INFORM 4*:955 (1993).
15. Dugan, L.R., B.W. Beadle and A.S. Henick, *J. Am. Oil Chem. Soc. 26*:681 (1949).
16. Privett, O.S., W.O. Lundberg, N.A. Khan, W.E. Tolberg and D.H. Wheeler, *Ibid. 30*:61 (1953).
17. *DX Advanced Operations Manual*, Nicolet Instrument Inc., Madison, 1988.
18. Conley, R.T., *Infrared Spectroscopy*, Allyn and Bacon, Boston, 1966.
19. Silverstein, R.M., and G.C. Bassler, *Spectrometric Identification of Organic Compounds*, John Wiley & Sons, New York, 1967.
20. Brown, C.W., P.F. Lynch, R.J. Obremski and D.S. Lavery, *Anal. Chem. 54*:1472 (1982).
21. Crocombe, R.A. M.L. Olson and S.L. Hill, in *Computerized Quantitative Infrared Analysis*, ASTM STP 934, edited by G.L. McClure, American Society for Testing and Materials, Philadelphia, 1987, pp. 95–130.
22. Fuller, M.P., G.L. Ritter and C.S. Draper, *Appl. Spectrosc. 42*:217 (1988).

[Received March 22, 1993; accepted December 27, 1993]